Available online at www.sciencedirect.com
SCIENCE DIRECT
Journal of Molecular Catalysis A: Chemical 243 (2006) 183–193
JOURNAL OF MOLECULAR CATALYSIS A: CHEMICAL
www.elsevier.com/locate/molcata

Al-MCM-41 supported phosphotungstic acid: Application to symmetrical and unsymmetrical ring opening of succinic anhydride

K. Usha Nandhini, Banumathi Arabindoo, M. Palanichamy, V. Murugesan *

Department of Chemistry, Anna University, Chennai 600025, India

Received 31 January 2005; received in revised form 11 August 2005; accepted 22 August 2005
Available online 23 September 2005

Abstract

Mesoporous Al-MCM-41 (Si/Al = 20) molecular sieve was synthesized hydrothermally and characterized by X-ray diffraction (XRD), nitrogen-sorption studies and ^{27}Al and ^{29}Si MAS-NMR spectroscopies. 10, 20 and 40 wt% phosphotungstic acid (PW) ($H_3PW_{12}O_{40}$) were supported on Al-MCM-41 and the resulting catalysts were characterized by XRD, FT-IR, nitrogen-sorption, DRIFT, ^{1}H and ^{31}P MAS-NMR and DRS UV–vis spectral techniques. ^{1}H MAS-NMR spectra of PW/Al-MCM-41 revealed leveling of the acidity of PW protons to Al-MCM-41. Their catalytic activities were evaluated in the esterification of succinic anhydride with ethanol in the temperature between 60 and 120 °C. Monoethyl succinate (MES) and diethyl succinate (DES) were obtained as products. The effects of alcohol/anhydride molar ratio and temperature were studied. Unsymmetrical alcoholysis of succinic anhydride with methanol and 1-butanol was also carried out successfully.

Keywords: Al-MCM-41 (20); Al-MCM-41 supported phosphotungstic acid; ^{1}H MAS-NMR; Esterification; Diethyl succinate; Unsymmetrical alcoholysis

1. Introduction

Organic esters are important intermediates in the synthesis of fine chemicals, drugs, plasticizers, food preservatives, pharmaceuticals, cosmetics and auxiliaries [1]. They are produced by homogeneously catalyzed batch process in industries using mineral acid catalyst such as hydrofluoric acid and sulphuric acid [2] or Lewis acid catalysts like tin octoate [3]. Mineral acid catalysts are corrosive, non-recyclable and need to be neutralized for disposal after the reaction. Lewis acid catalysts require careful removal after the reaction by adsorption on bleaching earth, which also produces large amount of waste. Hence, there is a need for ecofriendly and heterogeneous versatile processes [4]. Many heterogeneous catalysts such as ion-exchange resin [5], H-ZSM-5 [6], HY [7,8], triolic acid [9], sulphated oxides [10–12], hydrous zirconium oxide [13] and supported heteropolyacids [14] have been reported for esterification. But even these heterogeneous catalysts have problems; for instance, though zeolites possess high activity, they give a variety of undesired by-products [15]. Heteropolyacids exhibit nearly comparable activity as that of sulphuric acid in acid catalyzed reactions in the liquid phase [16,17], but unfortunately they are soluble in polar medium, which makes them difficult to separate from the reaction products. Hence, there has been interest in using supported HPAs, which resulted in the preparation of a family of HPA supported catalysts. In addition to the increased dispersion, supported HPAs inhibit coke formation during the reactions [18,19]. Reports are also available on zeolites supported heteropolyacids [20,21]. More recent studies on esterification reactions using heteropolyacids supported on MCM-41 [22] suggest that the formation of water during the reaction can result in re-dispersion of HPA on the surface [19]. Activated carbon supported polytungstic acid has shown excellent activity towards esterification of acetic acid with ethanol and 1-butanol [23,24]. Based on these reports esterification of succinic anhydride (SA) with ethanol has been studied over phosphotungstic acid supported on mesoporous Al-MCM-41 (20). The high aluminium content present in Al-MCM-41 (20) will provide its hydrophilic property to entrap more number of Keggin units thereby increasing the acidity of the resultant solid acid catalyst. The product diethyl succinate is used as a carrier in fragrances and in the manufacture of pharmaceuticals, agrochemicals and other organic compounds.

* Corresponding author. Tel.: +91 44 22301168; fax: +91 44 22200660.
E-mail address: v_murugu@hotmail.com (V. Murugesan).

1381-1169/$ – see front matter © 2005 Elsevier B.V. All rights reserved.
doi:10.1016/j.molcata.2005.08.028

2. Experimental

2.1. Catalyst preparation

Al-MCM-41 (Si/Al = 20) was synthesized hydrothermally using the gel composition: SiO_2:9.0EtOH:0.025Al_2O_3: 0.20CTAB:160H_2O. In a typical synthesis, 10.6 g sodium metasilicate and 0.6 g aluminium sulphate were dissolved in 60 g water and the resulting mixture was stirred vigorously until a clear solution was obtained. 3.36 g cetyltrimethylammonium bromide (CTAB) was dissolved in 20 ml ethanol. Thereafter, the solution containing sodium metasilicate and aluminium sulphate was added dropwise to the surfactant solution and the mixture was stirred for 1 h at room temperature. Then, 7.06 g 4N H_2SO_4 was added to the resulting gel so as to reduce the pH to ca. 11 and the stirring was continued for 3 h. The resultant homogeneous solution was transferred into a 300 ml stainless steel autoclave, sealed and heated in a hot air oven at 145 °C for 12 h. After cooling to room temperature, the resultant solid was recovered by filtration, washed several times with deionized water and dried in an oven at 100 °C for 6 h. Finally, the material was calcined at 550 °C in air for 6 h in order to remove the template from the mesopores.

Catalysts with different loadings of $H_3PW_{12}O_{40}\cdot xH_2O$ (PW, E-Merck GR Grade, Germany) on Al-MCM-41 were prepared by stirring the suspension of 1.0 g Al-MCM-41 in 10 ml methanol containing 0.1, 0.2 or 0.4 g PW at room temperature for 22 h [25]. The resultant mixture was dried at 80 °C and calcined at 200 °C for 2 h. This method facilitated the retention of all added PW in the support.

2.2. Physicochemical characterization

The powder X-ray diffraction (XRD) patterns of calcined Al-MCM-41 and PW/Al-MCM-41 catalysts were collected on a Siemens D 5005 diffractometer using nickel-filtered Cu Kα ($\lambda = 0.154$ nm) radiation. The diffractograms were recorded in the 2θ range 0.8–50° with a 2θ step size of 0.01° and a step time of 10 s at each point. Surface area measurement of all the catalysts was carried out by nitrogen adsorption at 77 K with an ASAP-2010 porosimeter from Micromeritics Corporation (Norcross, GA, USA). Before nitrogen adsorption–desorption measurements, the samples were outgassed for 3 h at 250 °C under vacuum ($p < 10^{-5}$ mbar) in the degas port of the adsorption analyzer. The specific surface area of the samples was calculated using the BET model. Pore size distributions were obtained from the desorption branch of the isotherms using the corrected form of Kelvin equation by means of the Barrett–Joyner–Halenda method as proposed by Kruk et al. [26].

Solid-state MAS-NMR spectrum of Al-MCM-41 was recorded on a Bruker DSX 300 spectrometer equipped with a magic angle spinning (MAS) unit and a magnetic field strength of 7.04 T. The spinning rates were 8 and 7 kHz and the resonating frequencies were 78.2 and 59.6 MHz for Al and Si, respectively. Spectral widths were 864.59 and 878.18 ppm for Al and Si, respectively. The external reference was aluminium nitrate for Al and tetramethylsilane (TMS) for Si. The experimental details for ^{31}P MAS-NMR were as follows: spinning rate 7 kHz; resonating frequency 121.5 MHz; spectral width 1261.15 ppm and external reference phosphoric acid. ^{1}H MAS-NMR spectra were recorded on a Bruker Avance 400 spectrometer operating at 400 MHz. A zirconia rotor (4 mm outer diameter) was spun at 10 kHz. The spectra were recorded by accumulating 16 scans with a $\pi/2$ pulse duration of 10 μs and repetition time of 8 s. The chemical shifts were with reference to TMS.

Diffuse reflectance UV–vis spectra of the catalysts were recorded on a Perkin-Elmer Lambda 18 spectrophotometer equipped with a Praying–Mantis diffuse reflectance attachment. $BaSO_4$ was used as the reference. FT-IR spectra of the samples were recorded on a Nicolet (Avatar 360) instrument using the KBr pellet technique by making 50 scans at 2 cm^{-1} resolution. About 15 mg of the sample was pressed (under a pressure of 2 tons cm^{-2}) into a self-supported wafer of 13 mm diameter. For acidity measurements, about 10 mg of the catalyst was placed in the sample holder and outgassed at 300 °C for 1 h in vacuum (10^{-5} mbar) and then cooled to ambient temperature followed by pyridine adsorption at the same temperature until equilibration. The catalyst was then evacuated at different temperatures (100–250 °C) under vacuum (10^{-5} mbar) for 30 min. The acidity was measured on the basis of IR spectrum of the adsorbed pyridine. Pyridine concentration of Brønsted and Lewis sites was calculated by measuring the integrated absorbance of bands representing pyridinium ion formation and coordinatively bonded pyridine [27,28] and by using correlations developed for porous aluminosilicates at 150 °C [29].

2.3. Catalytic studies

Esterification of succinic anhydride with ethanol was carried out in liquid phase. Succinic anhydride (1 mol), ethanol (1 or 2 mol) and catalyst (0.1 g) were taken in a 25 ml round-bottomed flask fitted with a reflux condenser. The flask with its contents was heated at a constant temperature in an oil bath and stirred magnetically. Aliquots of the hot mixture were withdrawn at regular intervals to monitor the progress of the reaction. The samples were centrifuged and the centrifugate were analyzed with a Shimadzu GC-17A gas chromatograph using a DB-5 capillary column (30 m × 0.25 mm × 0.25 μm) equipped with a flame ionization detector. The second alcohol was added at the end of 3 h of the reaction for unsymmetrical alcoholysis and the progress of the reaction was monitored as usual. The identification of the products was made using a GC–MS Perkin-Elmer Auto System XL gas chromatograph (Perkin-Elmer elite series PE-5 capillary column, 30 m × 0.25 mm × 1 μm) equipped with a Turbo Mass Spectrometer (EI, 70 eV) with helium as carrier gas at a flow rate of 1 ml/min.

3. Results and discussion

3.1. Characterization

3.1.1. XRD

XRD patterns of Al-MCM-41 and PW/Al-MCM-41 are shown in Fig. 1. Al-MCM-41 has the typical XRD pattern

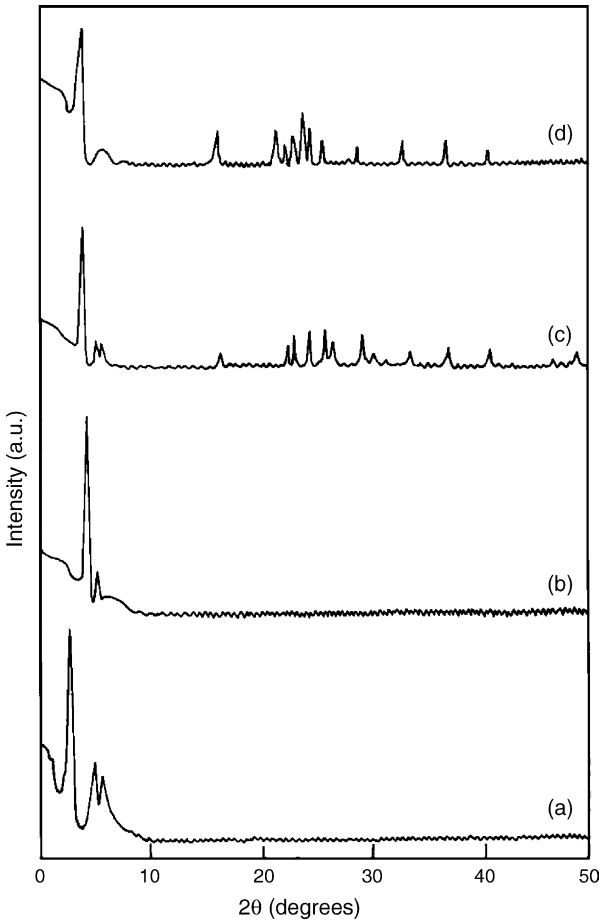

Fig. 1. XRD patterns of: (a) Al-MCM-41 (20), (b) 10 wt% PW/Al-MCM-41, (c) 20 wt% PW/Al-MCM-41 and (d) 40 wt% PW/Al-MCM-41.

exhibiting an intense peak at 2.24° (2θ) due to (1 0 0) plane and weak peaks at 4.06 and 4.68° due to higher order reflections (1 1 0) and (2 0 0) which are indexed to hexagonal lattice as reported by earlier workers [30,31]. The (1 0 0) plane reflection has been shifted to higher values of 2θ at 2.34° for 10, 20 and 40 wt% PW/Al-MCM-41, which is an indication of pore size decrease illustrating maximum use of PW to construct the Keggin phase within the pores. However, the intensity of peak decreases upon increasing PW loading and lines appear above 20° (2θ) corresponding to the crystalline PW phase. Comparison of the XRD patterns of pristine Al-MCM-41 and PW/Al-MCM-41 reveals that the mesoporous structure is rather intact even after the loading of PW. The XRD patterns revealed that at low loadings of PW (below 20 wt%) no distinct diffraction peaks due to HPA crystallites are observed. But when the loading exceeded above 20 wt% broad diffraction peaks appeared at 2θ = 20° characteristic of solid-state PW [32]. For 20 and 40 wt% loadings there exists a larger number of Keggin units inside the pores and also on the walls outside the pores interacting with the framework. Hence, for the Keggin units present outside the pores we can expect the corresponding XRD peaks, which appear as a very small peaks compared to the peak due to (1 0 0) plane. The peaks are neither very much sharp nor intense in the present study. Hence, it is suggested that most of the PW

Table 1
Physicochemical characteristics of the catalysts

Catalyst	d_{100} (Å)	S_{BET} (m^2/g)	Pore diameter (Å)	Pore volume (cm^3/g)
Al-MCM-41 (20)	39.39	1223	24.3	0.82
10 wt% PW/Al-MCM-41	37.75	980	21.8	0.69
20 wt% PW/Al-MCM-41	38.12	860	22.5	0.52
40 wt% PW/Al-MCM-41	38.12	770	22.5	0.44

crystallizes inside the pores of the support. The d_{100} spacing derived from XRD and surface area, pore diameter and pore volume derived by the BET method for pristine Al-MCM-41 and PW/Al-MCM-41 catalysts are presented in Table 1. The d spacing is less for PW loaded Al-MCM-41 than for pristine Al-MCM-41. This observation reveals pore size contraction as a consequence of lining of mesoporous channel by a PW film. Among the PW loaded catalysts the decrease in d spacing for 20 and 40 wt% PW/Al-MCM-41 is less than for 10 wt% PW/Al-MCM-41. This observation suggests enhanced usage of PW in the construction of Keggin structure in 20 and 40 wt% PW/Al-MCM-41 compared to 10 wt% loaded catalyst. These details are also very well reflected in the pore diameter and pore volume of PW/Al-MCM-41 catalysts. The pore diameter of 10 wt% PW/Al-MCM-41 catalyst is smaller than that of both 20 and 40 wt% PW/Al-MCM-41 catalysts, which is in line with our view. The pore diameter is also only 10% smaller than that of pristine Al-MCM-41 and therefore it is presumed to be present as a uniform film or as a monolayer coverage. The presence of such a type of layer was also discussed by Liu et al. [33]. Thus, the decrease in pore volume for the loaded catalyst compared to pristine Al-MCM-41 evidently proves the formation of the PW film and/or the Keggin phase within the pores of Al-MCM-41. The gradual decrease in the pore volume with increase in PW loading also confirms the formation of bulk Keggin phase within the pores of 20 and 40 wt% PW/Al-MCM-41 catalysts.

3.1.2. Nitrogen adsorption studies

Nitrogen adsorption isotherms of pristine Al-MCM-41 and PW/Al-MCM-41 catalysts are shown in Fig. 2. Each isotherm

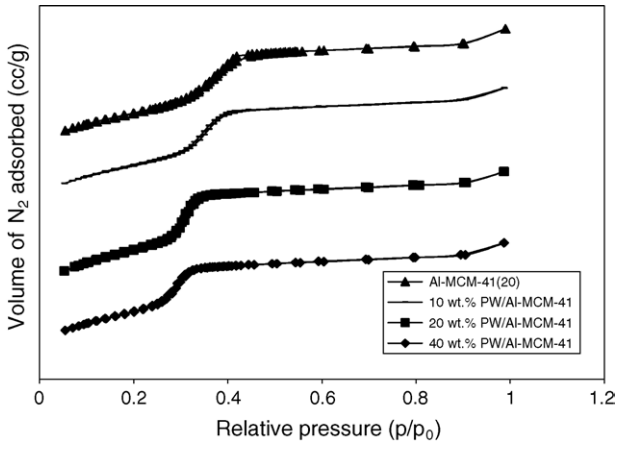

Fig. 2. Nitrogen adsorption–desorption isotherms of Al-MCM-41 and 10, 20 and 40 wt% PW/Al-MCM-41 catalysts.

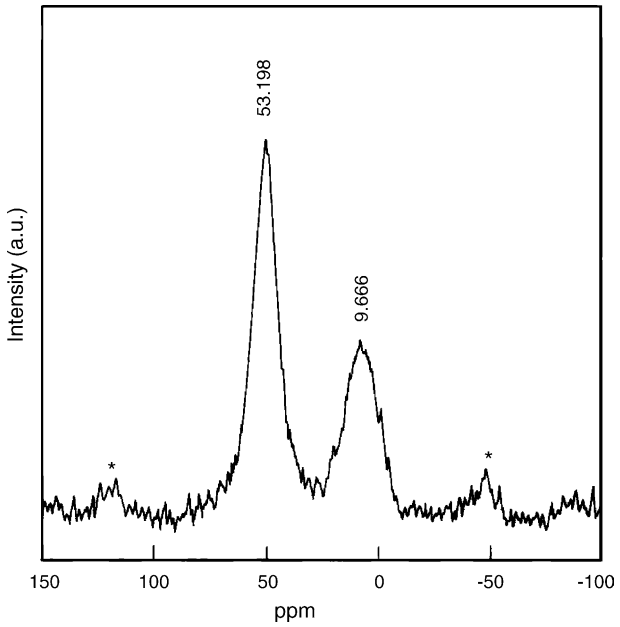

Fig. 3. ^{27}Al MAS-NMR spectrum of calcined mesoporous Al-MCM-41 (20).

shows type IV character typical of mesoporous MCM-41. All materials exhibit a steep rise commencing at ca. $p/p_0 = 0.27$–0.32 due to capillary condensation of nitrogen in the mesopores of ca. 2.1–2.5 nm diameter [34]. The specific surface area of samples from the BET method ranges between 1223 and 770 m^2/g (Table 1).

3.1.3. ^{27}Al and ^{29}Si MAS-NMR

The incorporation of aluminium into the framework of Al-MCM-41 was analyzed by ^{27}Al MAS-NMR spectroscopy and the spectrum of the calcined Al-MCM-41 is shown in Fig. 3. The spectrum shows a sharp resonance peak at $\delta = 53.2$ ppm which is assigned to tetrahedrally coordinated framework aluminium [35]. A broad and low intense peak at $\delta = 9.6$ ppm suggests the presence of octahedral non-framework aluminium species [36]. Generally, materials with high aluminium contents are susceptible to leaching of framework aluminium during calcination [34]. Since calcination of as-synthesized materials was done in air directly without using nitrogen in the beginning, this might have caused leaching of framework aluminium. ^{29}Si MAS-NMR spectrum of the calcined Al-MCM-41 catalyst is shown in Fig. 4. Four different silicon sites can be classified using the notation Q^n (mAl) which denotes a central silicon atom abound to 'n' next-nearest silicon or aluminium atoms, out of which 'm' sites are aluminium. In the present case the peak at $\delta = -108.6$ ppm is assigned to Q^4 sites (four tetrahedral neighbours) and the peaks at $\delta = -103.0$ ppm and low values appearing as shoulders are assigned to Q^3 Si(1Al) and Q^2 sites, respectively [37].

3.1.4. ^{1}H MAS-NMR

Fig. 5 depicts ^{1}H MAS-NMR spectra of Al-MCM-41 and PW/Al-MCM-41 catalysts. Weak signals at 1.1 and 1.5 ppm are assigned to the defective Si–OH groups as reported by Mastikhin et al. [38]. The intense peak at 4.77 ppm is assigned to Brønsted acid sites based on the spectrum of Hβ zeolite as shown in the

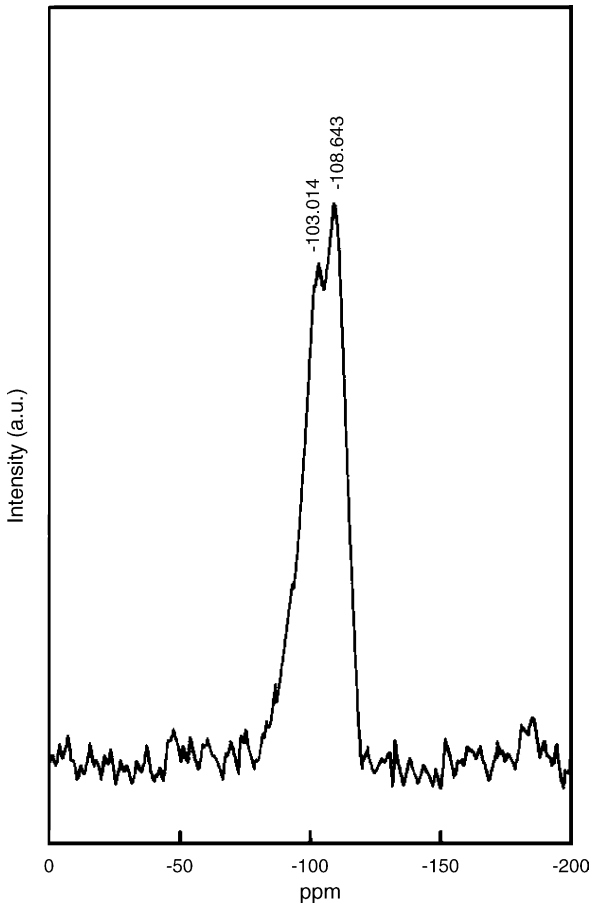

Fig. 4. ^{29}Si MAS-NMR spectrum of calcined mesoporous Al-MCM-41 (20).

same figure [39]. The Gaussian appearance without any shoulder demonstrates nearly similar type of Brønsted acid sites on the catalyst surface which is contradictory to the previous reports, which states acid sites of different strengths on the surface of Al-MCM-41 [40–42]. The leveling of acid strength may be due to

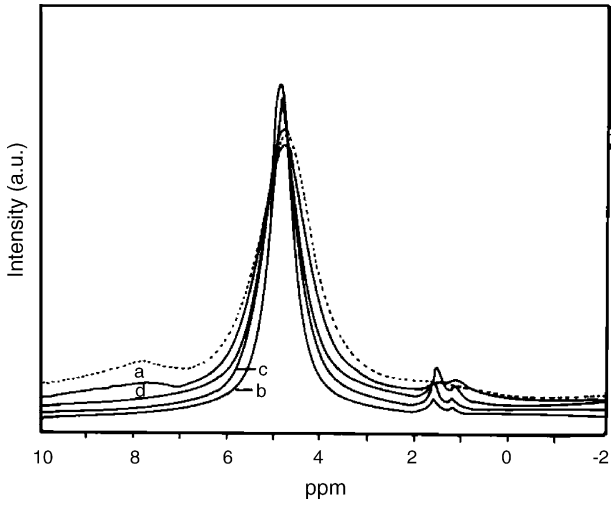

Fig. 5. ^{1}H MAS-NMR spectra of: (a) Al-MCM-41 (20), (b) 10 wt% PW/Al-MCM-41, (c) 20 wt% PW/Al-MCM-41 and (d) 40 wt% PW/Al-MCM-41.

the low Si/Al ratio of the catalyst. The ^{1}H MAS-NMR spectrum of 10 wt% PW/Al-MCM-41 shows an intense and sharp signal at 4.77 ppm. The peak appears very narrow in comparison to that of Al-MCM-41 demonstrating nearly the same environment of protons when loaded with PW. ^{1}H MAS-NMR spectrum of PW generally displays a characteristic signal at 9.3 ppm [38,43]. But this signal is absent in the present spectrum and hence the acidity of PW protons gets equalized to that of Al-MCM-41. Similar observation has been already reported for PW/MCM-41 by Jalil et al. [43]. They have also reported a new signal around 3 ppm due to newly generated protons. Such upshifted signal is not observed in the present materials. Hence, such protons originated by the modification of defective Si–OH groups are not formed in this catalyst. But the signals due to defective sites between 1 and 2 ppm appears more resolved for loaded catalysts compared to those of Al-MCM-41 catalyst. Hence, acidity of some of the defective –OH groups are considered to be modified as that of Brønsted acid sites which produce a signal at 4.77 ppm. Certainly there might be condensation of very close defective –OH groups. From these observations, it is confirmed that PW is not present as a separate entity on the catalyst surface but interacting with Al-MCM-41. The spectra of 20 and 40 wt% PW/Al-MCM-41 presents similar features. An important point to be emphasized in all the spectra of PW loaded catalyst is the increase in intensity of the signal due to defective –OH sites. Hence, there might be breaking of some type of bridges into fresh Si–OH groups. Hence, the present study unambiguously establishes the crystallization of the Keggin phase, particularly inside the pores of Al-MCM-41, which becomes a novel, convenient and effective support for PW. The failure of crystallization outside the pores of Al-MCM-41 also suggests strong interaction between Al-MCM-41 and PW within the pores.

3.1.5. ^{31}P MAS-NMR

^{31}P MAS-NMR is the most effective method for examining the state of phosphorous in heteropolyacids [44]. Fig. 6 shows ^{31}P MAS-NMR spectra of 10, 20 and 40 wt% loaded PW/Al-MCM-41 catalysts. The PW/Al-MCM-41 catalysts with high PW content (20 and 40 wt%) exhibit a sharp resonance at −15.2 ppm, which is close to that of bulk PW [45]. This indicates unambiguously that the Keggin structure is retained even after PW is loaded on Al-MCM-41. In contrast, the spectra of PW/Al-MCM-41 with low PW content show partial decomposition of the Keggin structure. Thus the spectrum of 10 wt% PW/Al-MCM-41 shows a resonance of low intensity at −13.1 ppm besides the intense line of PW. This line may well be assigned to lacunary heteropoly anions such as $PW_{11}O_{39}^{7-}$ and $P_2W_{17}O_{61}^{10-}$ or unsaturated anions like $P_2W_{18}O_{62}^{6-}$ and $P_2W_{21}O_{71}^{6-}$ [45], which can be formed by decomposition of the PW Keggin structure.

3.1.6. DRS

The diffuse reflectance (DRS) UV–vis spectra of bulk PW and PW/Al-MCM-41 were recorded to understand the nature of species present on the support (Fig. 7). The spectra show two peaks, one at 260 nm and another in the range 315–320 nm suggesting the presence of undegraded $H_3PW_{12}O_{40}$ species on the support [46]. In other words, the Keggin phase remains intact upon loading PW on Al-MCM-41.

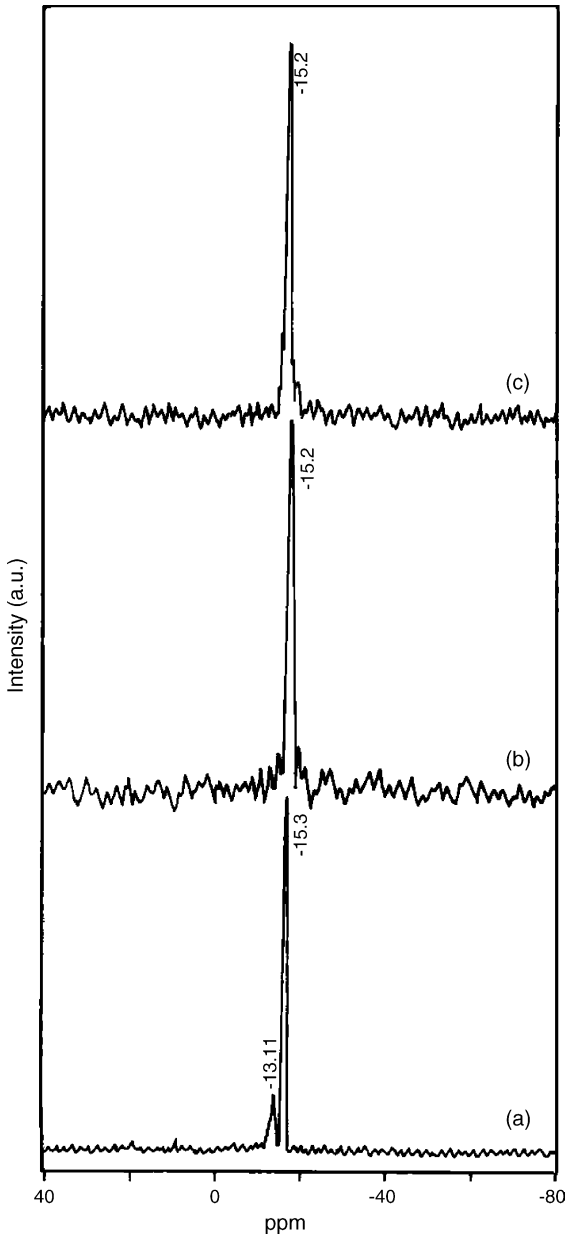

Fig. 6. ^{31}P MAS-NMR spectra of: (a) 10 wt% PW/Al-MCM-41, (b) 20 wt% PW/Al-MCM-41 and (c) 40 wt% PW/Al-MCM-41.

3.1.7. FT-IR

FT-IR spectra were recorded for supported PW samples in order to confirm the presence of Keggin anion on Al-MCM-41 surface. The $PW_{12}O_{40}^{3-}$ Keggin ion structure consists of a PO_4 tetrahedron surrounded by four W_3O_{13} groups formed by edge-sharing octahedra. These groups are connected to each other by corner-sharing oxygen [44]. This structure gives rise to four types of oxygen which is responsible for the finger print bands of Keggin ion between 1200 and 700 cm^{-1}. The bands at 1080 and 984 cm^{-1} are due to P–O and W=O vibrations, respectively. The corner-shared and edge-shared vibrations of W–O–W bands appear at 892 and 800 cm^{-1}, respectively [45,47]. Fig. 8

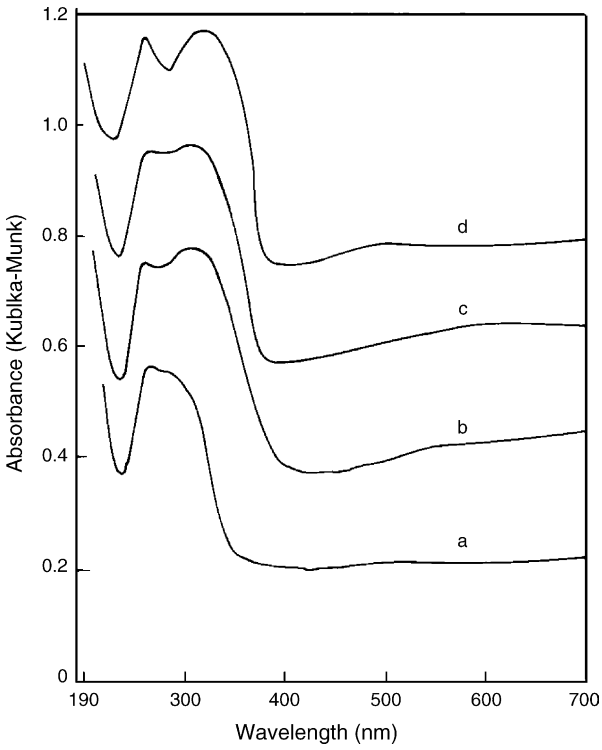

Fig. 7. UV–vis DRS spectra of: (a) 10 wt% PW/Al-MCM-41, (b) 20 wt% PW/Al-MCM-41, (c) 40 wt% PW/Al-MCM-41 and (d) pure PW.

reveals typical bands of Keggin absorption at 1091, 968, 896 and 802 cm^{-1}. These spectral features remain the same irrespective of PW loadings. A gradual increase in the absorbance of W–O–W corner-shared vibrations at 892 cm^{-1} is observed for Al-MCM-41 supported PW catalysts. This could indicate that significant amount of Keggin phase starts to form only at and above 20 wt% loading of PW.

3.1.8. Pyridine adsorbed FT-IR

FT-IR spectra of supported catalysts were recorded after adsorption with pyridine, followed by evacuation at elevated temperatures (Fig. 9). The spectra show contribution of pyridine adducts in the region 1650–1450 cm^{-1}. The formation of pyridinium ion as shown from the absorption at 1545 and 1490 cm^{-1}

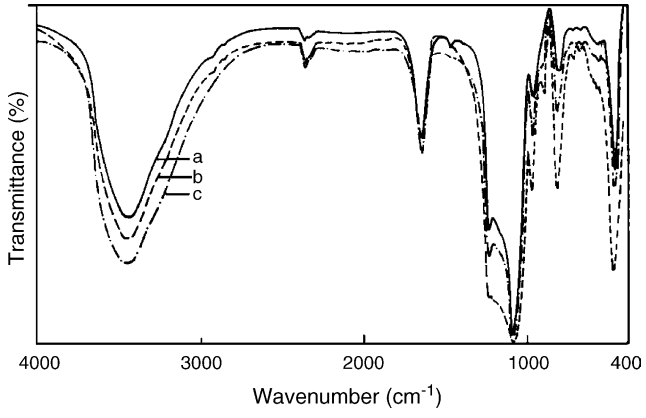

Fig. 8. FT-IR spectra of: (a) 10 wt% PW/Al-MCM-41, (b) 20 wt% PW/Al-MCM-41 and (c) 40 wt% PW/Al-MCM-41.

is characteristic of Brønsted acid sites and both Brønsted and Lewis acid sites, respectively [48,49]. The band at 1634 cm^{-1} is due to ring vibration of pyridine bound to Brønsted acid sites [39]. The bands at 1445 and 1613 cm^{-1} are assigned to hydrogen-bonded pyridine [39,41,50] which are characteristics of Lewis acid sites. PW reacts with the support by breaking the Si–O–Al bridge with liberation of water. Phosphorus is attached to silicon through oxygen as shown in Scheme 1. Thus, Al becomes tri-coordinated, exhibiting Lewis acid properties. This interaction depends on the level of PW loading. Above 20 wt% PW monolayer covers the surface of support [33,48] and further addition of PW will result in agglomeration thus preventing additional active sites to generate Lewis acidity. Hence, there is a decrease in Lewis acidity. Such type of interactions has been reported to increase the hydrothermal stability of ZSM-5 with H_3PO_4 and alkyl phosphine compounds [51]. Comparison of spectra reveals that 20 wt% PW/Al-MCM-41 possess greater amount of acid sites (B and L acid sites) than other catalysts as the corresponding bands in the former are more intense than those of the latter. The bands at 1613, 1490 and 1445 cm^{-1} reduce at elevated temperatures for all the catalysts but the band at 1545 cm^{-1} remains almost the same, particularly in the case of 20 wt% PW/Al-MCM-41 indicating strong Brønsted acid sites of the catalyst. The decrease in the intensity of the absorption band at 1445 cm^{-1} indicates diminishing nature of physisorbed pyridine after evacuation at elevated temperatures [28,52]. The DRIFT spectra of desorption of adsorbed pyridine over PW/Al-MCM-41 at 100, 150 and 250 °C were taken between 400 and 4000 cm^{-1} [25]. Pyridine could be adsorbed on acid sites as pyridinium ion and also as pseudo-liquid phase, while most of the pseudo-liquid phase pyridine has been removed when evacuated at 80 °C [52]. In the present study, the concentration of Brønsted and Lewis acid sites was calculated after evacuation at 150 °C using the extinction co-efficient of the bands of Brønsted and Lewis acid sites adsorbed pyridine [29] and the acidity values are presented in Table 2. As the pyridine adsorbed by pseudo-liquid phase behaviour (physisorbed) has been removed at 150 °C, the strong Brønsted acid sites only be retained which indicates the strong acidity of the catalyst [53]. The data in the table also indicates the presence of high amount of Brønsted and Lewis acid sites present in 20 wt% PW/Al-MCM-41. From the B/L ratio, it is found that 20 wt% PW/Al-MCM-41 possesses high value thus indicating the presence of strong acid sites compared to other catalysts. Hence, the acidity of the catalysts follows the order: 20 wt% PW/Al-MCM-41 > 40 wt% PW/Al-MCM-41 > 10 wt% PW/Al-MCM-41 > Al-MCM-41.

3.2. Catalytic studies

Esterification of succinic anhydride with ethanol was studied over Al-MCM-41, 10, 20 and 40 wt% PW/Al-MCM-41 with a feed ratio 1:2 (succinic anhydride:ethanol) at 60, 80, 100 and 120 °C. The results are shown in Table 3. As in the case of phthalic and maleic anhydrides monoesterification [23,54], the succinic anhydride monoesterification was also fast and independent of the catalyst. The conversion of succinic anhydride was 100% even at the end of 3 h of the reaction. Subsequent

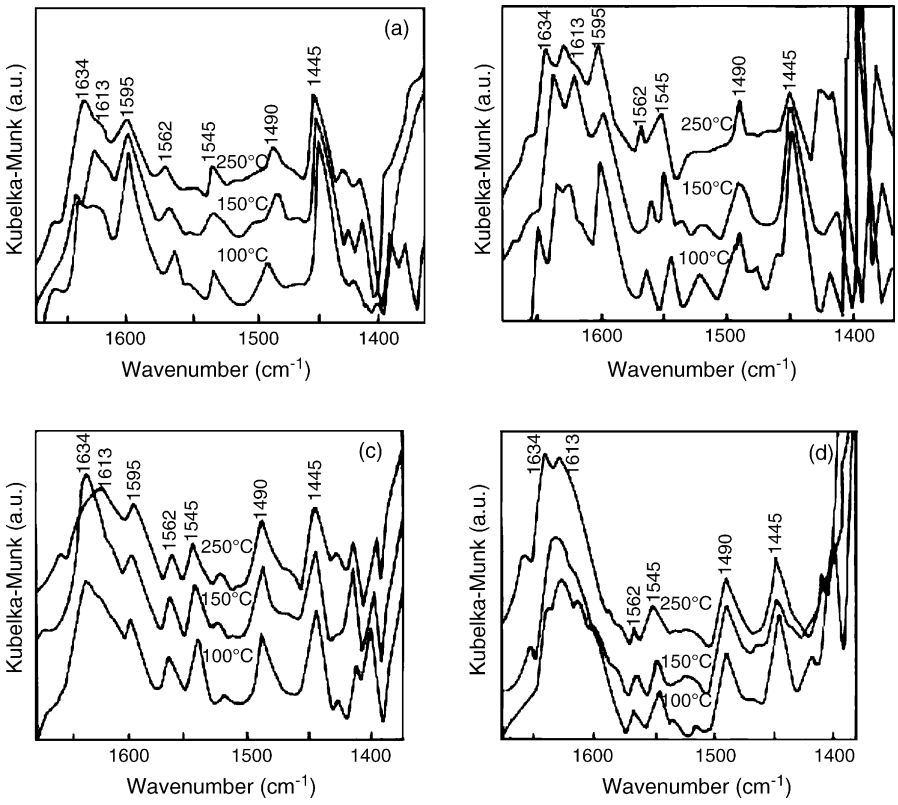

Fig. 9. DRIFT spectra of pyridine adsorption over: (a) Al-MCM-41 (20), (b) 10 wt% PW/Al-MCM-41, (c) 20 wt% PW/Al-MCM-41 and (d) 40 wt% PW/Al-MCM-41.

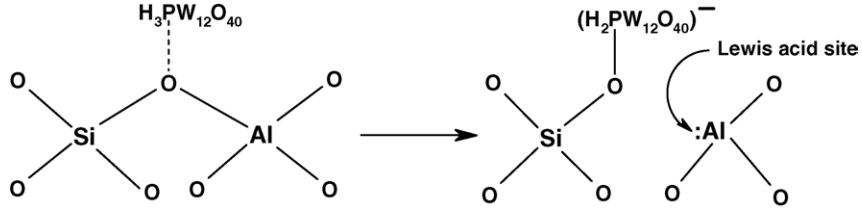

Scheme 1.

esterification of monoethyl succinate (MES) to diethyl succinate (DES) was found to be slow and dependent on the catalyst as evident from the data in Table 4. The amount of MES decreased gradually with increase in time over all the catalysts at all temperatures. Rapid decrease in the amount of MES was observed with increase in temperature. As MES can only yield DES, the decrease in the amount of MES with increase in time corresponds to increase in the yield of DES at each time interval. Twenty weight percent PW/Al-MCM-41 gives higher yield of DES than either 40 or 10 wt% PW/Al-MCM-41 catalyst at the end of 12 h of the reaction. The low yield over 40 wt% PW/Al-MCM-41 might be attributed to diffusional constraint of MES into the pores in lieu of large size of the PW Keggin phase [24]. The low activity of 40 wt% of PW/Al-MCM-41 is due to the uniform layer formation of PW in the mesopores, which masks the active sites for the reaction. The large size of the Keggin

Table 2
Brønsted and Lewis acidity values for Al-MCM-41 and PW/Al-MCM-41

Catalyst	Brønsted (B) acid site concentration (mmol/g)	Lewis (L) acid site concentration (mmol/g)	B/L acid site ratio
Al-MCM-41	0.12	0.18	0.66
10 wt% PW/Al-MCM-41	0.17	0.24	0.71
20 wt% PW/Al-MCM-41	0.25	0.32	0.78
40 wt% PW/Al-MCM-41	0.20	0.27	0.74

Desorption temperature = 150 °C.

Table 3
Effect of feed ratio on the yield of DES

Time (h)	Feed ratio (SA: EtOH)					
	1:1		1:2		1:3	
	Amount of MES (%)	Yield of DES (%)	Amount of MES (%)	Yield of DES (%)	Amount of MES (%)	Yield of DES (%)
3	95.7	4.3	70.4	29.5	73.8	26.1
6	95.0	5.0	54.5	45.5	61.9	38.1
9	93.5	6.5	46.8	53.2	59.5	40.5
12	93.0	7.0	33.1	66.9	60.0	43.0

Catalyst = 20 wt% PW/Al-MCM-41 (20); temperature = 120 °C; catalyst weight = 0.1 g.

structure is shown by XRD, surface area and pore volume analyses (Table 1). Ten weight percent PW/Al-MCM-41 shows low yield due to less amount of Keggin phase.

In order to examine the catalytic activity of the support, viz. Al-MCM-41, the reaction was carried over Al-MCM-41 under identical conditions. It is observed that the support Al-MCM-41 exhibited the low activity at all temperatures. Since the catalyst possesses sufficient density of acid sites it may be expected to exhibit comparable activity as that of PW loaded Al-MCM-41 catalysts. The low activity of Al-MCM-41 is attributed to the formation of water clusters around Brønsted acid sites by the released water. The present study reveals that 20 wt% PW/Al-MCM-41 is more active than the others. When the yield of DES is correlated with increase in temperature for all the catalysts, a non-linear variation is evident. Such a non-proportionate increase at 120 °C may be attributed to activation of water that reverts DES to MES.

3.2.1. Effect of feed ratio

The effect of feed ratio on the yield of DES was examined over 20 wt% PW/Al-MCM-41 and the results are presented in Table 3. The increase in the yield of DES is dramatic when the feed ratio is changed from 1:1 to 1:2. The low yield at the feed ratio of 1:1 is due to insufficient quantity of ethanol for nucleophilic attack on chemisorbed MES on the Brønsted acid sites of the catalyst. The high yield at the feed ratio of 1:2 evidently proves that the mechanism of esterification is of a Rideal–Eley type. Similar increase in the yield of DES is also expected for a feed ratio 1:3, but it decreases. This may be due to coverage of the catalyst with ethanol that prevents chemisorption of MES. Based on this result it could be discerned that the reaction does not proceed via chemisorption of alcohol to produce alkyl cation and its subsequent reaction with MES to yield DES. The absence of protonation of alcohol was also verified by running the probe reaction separately: the alkylation of very reactive substrate, namely phenol, with ethanol over 20 wt% PW/Al-MCM-41 with a feed ratio 1:3 at 120 °C resulted in no ethylation.

3.2.2. Unsymmetrical alcoholysis

Unsymmetrical alcoholysis of cyclic anhydride is a reaction of recent research interest. Such unsymmetrical alcoholysis has been successfully applied to maleic anhydride [54]. In the

Table 4
Effect of temperature on the yield of DES on Al-MCM-41 and PW loaded Al-MCM-41

Catalyst	Time (h)	Temperature (°C)							
		60		80		100		120	
		Amount of MES (%)	Yield of DES (%)	Amount of MES (%)	Yield of DES (%)	Amount of MES (%)	Yield of DES (%)	Amount of MES (%)	Yield of DES (%)
10 wt% PW/Al-MCM-41	3	94.5	5.5	91.1	8.9	75.8	24.2	67.5	32.5
	6	93.6	6.4	82.1	17.9	65.7	34.3	59.6	40.4
	9	94.9	8.1	80.0	20.0	59.7	40.3	53.5	46.5
	12	89.3	10.7	74.0	26.0	53.1	46.9	47.9	52.1
20 wt% PW/Al-MCM-41	3	93.9	6.1	94.1	5.9	79.1	20.9	70.5	29.5
	6	91.3	8.7	87.0	13.0	67.2	32.8	54.5	45.5
	9	88.7	11.3	82.8	17.2	62.2	37.8	46.8	53.2
	12	88.6	11.4	75.7	24.3	57.0	43.0	33.1	66.9
40 wt% PW/Al-MCM-41	3	92.8	7.2	95.4	4.6	75.7	24.3	71.0	29.0
	6	91.5	8.5	93.0	7.0	64.3	35.7	59.9	40.1
	9	90.9	9.1	85.4	14.6	60.2	39.9	47.6	52.4
	12	86.8	13.2	79.0	20.9	59.7	40.7	49.5	50.5
Al-MCM-41 (20)	3	97.9	2.1	97.6	2.4	96.7	3.3	91.2	8.8
	6	97.8	2.2	97.3	2.7	96.2	3.8	88.5	11.5
	9	97.7	2.3	96.9	3.1	96.1	3.9	86.8	13.2
	12	95.3	4.7	96.2	3.8	95.5	4.5	84.9	15.1

Catalyst weight = 0.1 g; feed ratio (SA:EtOH) = 1:2.

Table 5
Unsymmetrical alcoholysis with ethanol and methanol

Feed ratio	Time (h)	SA conversion (%)	Amount of MES (%)	Yield (%)		
				DES	MMS	Me.Et.S
(SA:EtOH:MeOH) (1:1:1)	3	95.2	90.1	5.1	–	–
	6	96.5	17.4	6.8	2.3	70.1
	9	97.6	14.5	7.6	3.5	72.0
	12	98.6	11.7	8.7	4.6	73.6
(SA:EtOH:MeOH) (1:1:3)	3	96.0	90.3	5.7	–	–
	6	96.8	16.2	6.0	2.6	70.6
	9	97.0	14.0	6.5	3.8	72.8
	12	98.0	12.7	6.5	5.1	73.7

Catalyst = 20 wt% PW/Al-MCM-41; temperature = 120 °C.

present study succinic anhydride has been chosen for unsymmetrical alcoholysis/ring opening. Ethanolysis and methanolysis of succinic anhydride were carried out consecutively in the liquid phase over 20 wt% PW/Al-MCM-41 and the results are presented in Table 5. MES and DES were the only products observed at the end of 3 h of ethanolysis. Conversion of succinic anhydride was nearly 95% at the end of 3 h. The yield of MES was higher than DES since monoesterification is rapid and does not require catalyst as observed with maleic and phthalic anhydrides [23,54]. Moreover, the consecutive esterification of MES could occur only at the end of monoesterification as the concentration of ethanol is not sufficient enough to speed up the second esterification. The yield of unsymmetrical ester, methyl ethyl succinate (Me.Et.S), increased with increase in the reaction time. Monomethyl succinate (MMS) was obtained but dimethyl succinate (DMS) was not obtained since the former was present in very low amount.

As MES can react either in the eclipsed or staggered conformation with methanol, it is of interest to explore the exact conformation through which the reaction proceeds. Monoethyl succinate may be expected to remain in the eclipsed conformation so that the carboxyl group can have hydrogen-bonding interaction with the ester group. Under this condition the alkyl group in the ester can influence the incoming alcohol for nucleophilic reaction with the carboxyl group that remains in the protonated form. Since methanol closely matches the ethyl group of the ester in hydrophobicity, methanol is better attracted than 1-butanol in the esterification. The results in Tables 5 and 6 support this view. Although 1-butanol is more nucleophilic than methanol, the low yield of unsymmetrical ester butylethyl succinate (BES) is definitely due to mismatch of the hydrophobicity of the ethyl group of the ester and the butyl group of 1-butanol. In addition, 1-butanol with a boiling point of 117 °C has higher boundary barrier at 120 °C to escape than methanol (64 °C) in order to react with MES. But unsymmetrical alcoholysis with both alcohols is successful.

The reaction was also carried out with the increased amount of methanol and 1-butanol in the feed (1:1:3) and the results are presented in Tables 5 and 6. The yields of unsymmetrical esters with both alcohols are the same. But the yield of heteroesters with methanol at both feed ratios (1:1:1 and 1:1:3) is equal (73.6%). The same yield for both feed ratios supports the insignificant nature of boundary barrier in methanol. But there is a difference of about 10% in the yield of BES with 1-butanol for the change of the feed ratio from 1:1:1 to 1:1:3. Hence, the boundary barrier in this reaction is evident. In order to confirm

Table 6
Effect of unsymmetrical alcoholysis in the presence of 1-butanol

Feed ratio	Time (h)	SA conversion (%)	Yield (%)			
			MES	DES	MBS	BES
(SA:EtOH:BuOH)[a] (1:1:1)	3	95.0	90.1	4.9	–	–
	6	95.6	25.9	8.8	1.8	59.2
	9	96.7	23.8	9.4	2.2	61.3
	12	97.5	18.5	10.3	3.0	65.7
(SA:EtOH:BuOH)[a] (1:1:3)	3	95.6	90.2	5.4	–	–
	6	96.8	19.4	6.6	1.3	69.5
	9	97.0	16.4	7.3	1.8	71.5
	12	98.0	9.7	11.3	2.7	74.3
(SA:EtOH:BuOH)[b] (1:1:3)	3	95.1	90.4	4.7	–	–
	6	95.7	16.1	7.9	1.8	69.9
	9	96.2	11.0	8.5	2.5	74.4
	12	96.8	4.7	10.8	3.1	78.2

[a] Catalyst employed 20 wt% PW/Al-MCM-41.
[b] Catalyst employed 20 wt% PW/AlPO.

this, the reaction was also studied at 150 °C. The yield of BES has increased by 12% (not shown here) thus supporting the existence of boundary barrier.

In order to establish the influence of the support on unsymmetrical alcoholysis, the reactants succinic anhydride, ethanol and 1-butanol were mixed in the ratio 1:1:3, respectively, and the reaction was carried over 20 wt% PW/AlPO at 120 °C. The results are presented in Table 6. The same yield of BES over both the catalysts shows the absence of any significant role of the support in unsymmetrical alcoholysis. This may be due to significant masking and preventing of active sites of the support for the reaction.

3.2.3. Sustainability of 20 wt% PW/Al-MCM-41

In order to confirm that PW is not leached out from the support surface during the reaction, 20 wt% PW/Al-MCM-41 catalyst was recycled several times for the same reaction under similar reaction conditions. There is no appreciable change either in the conversion or products yield. Further, since it is a liquid-phase reaction the leached out PW will again be redispersed on the catalyst surface [19]. Verheof et al. [22] have reported sintering of PW phase in the esterification of hexanoic acid with 1-hexanol based on the appearance of new signals in the XRD of the spent catalyst. As reduction in the conversion and products yield remained minimal for several recycles of the reaction, such sintering is excluded in the present study. Moreover the presence of less intense peaks due to the Keggin phase is also found for 20 wt% PW/Al-MCM-41 in our study unlike the finely dispersed state proposed by Verheof et al. [22] which could promote sintering.

4. Conclusion

Al-MCM-41 supported phosphotungstic acid of different loadings were synthesized and characterized successfully. The characterization study revealed the retention of Keggin structure of PW on the Al-MCM-41 surface. Their catalytic activities towards esterification of succinic anhydride with ethanol showed rapid monoesterification of succinic anhydride and slow catalyst dependent subsequent esterification of monoethyl succinate to diethyl succinate. This characteristic behaviour is conveniently exploited to obtain unsymmetrical ester like methyl ethyl succinate and butyl ethyl succinate using methanol and 1-butanol, respectively, as the second alcohol source. The activities of 10, 20 and 40 wt% PW/Al-MCM-41 are found to be nearly comparable. Irrespective of the nature of the support, namely Al-MCM-41 or mesoporous AlPO, the catalytic activity of esterification of succinic anhydride depends on the amount of loading of PW. The unsymmetrical alcoholysis with methanol and 1-butanol as the second alcohol sources is successful and this technique can be exploited commercially for the production of unsymmetrical esters.

Acknowledgements

The authors gratefully acknowledge the financial support from DST, New Delhi, India (Sanction No. SP/S1/H–22/99), for this research work. One of the authors (K.U.) is grateful to CSIR, New Delhi, for the award of Senior Research Fellowship.

References

[1] J.G. Bushey, C.I. Eastman, A. Klingsberg, L. Spiro (Eds.), Enclyclopedia of Chemical Technology, vol. 9, Wiley, New York, 1972, p. 311.
[2] D. Jaques, J.A. Leisten, J. Chem. Soc. (1964) 2683.
[3] A. Kowalski, A. Duda, S. Penczok, Macromol. Rapid Commun. 19 (11) (1998) 567.
[4] R.A. Sheldon, J. Chem. Technol. Biotechnol. 68 (1997) 381.
[5] J. Gimenez, J. Costa, S. Cervera, Ind. Eng. Chem. Res. 26 (1987) 198.
[6] H.B. Zhang, B.-Z. Zhang, H.-X. Li, J. Nat. Gas. Chem. (1992) 49.
[7] A. Corma, H. Garcia, S. Iborra, J. Prinio, J. Catal. 120 (1989) 78.
[8] E. Santacesaria, D. Gelosa, P. Danise, S. Carra, J. Catal. 80 (1983) 427.
[9] Z.-H. Chen, T. Lizuka, K. Tanabe, Chem. Lett. (1984) 1085.
[10] M. Hino, K. Arata, Chem. Lett. (1981) 1671.
[11] F.S. Guner, A. Sirkecioglu, S. Yulmaz, A.T. Erciyes, A. Erdem-Senatalar, J. Am. Oil Chem. Soc. 73 (1996) 347.
[12] G. Lu, Appl. Catal. A 133 (1995) 11.
[13] K. Takahashi, M. Shibagaki, H. Matsushita, Bull. Chem. Soc. Jpn. 62 (1989) 2353.
[14] W. Chu, X. Yang, X. Ye, Y. Wu, Appl. Catal. A 145 (1996) 125.
[15] Y.Q. Li, Petrochem. Technol. 54 (1981) 309.
[16] M. Misono, T. Okuhara, N. Mizuno, Stud. Surf. Sci. Catal. 214 (1988) 267.
[17] I.V. Kozhevnikov, Russ. Chem. Rev. (English translation) 56 (1987) 811 (English translation).
[18] Y. Izumi, K. Urabe, M. Onaka, Zeolites, Clay and Heteropoly Acids in Organic Reactions, vol. 99, Kodansha/VCH, Tokyo, 1992, p. 99.
[19] K. Wilson, J.H. Clark, Pure Appl. Chem. 72 (7) (2000) 1313.
[20] K. Pamin, A. Kubacka, Z. Olejniczak, J. Haber, B. Sulikowski, Appl. Catal. A: Gen. 194–195 (2000) 137.
[21] J. Haber, K. Pamin, L. Matachowski, D. Mucha, Appl. Catal. A: Gen. 256 (2003) 141.
[22] M.J. Verheof, P. Kooyman, J.A. Peters, H. van Bekkum, Microporous Mesoporous Mater. 27 (1999) 365.
[23] M.A. Schwegler, H. van Bekkum, N.A. de Munck, Appl. Catal. 74 (1991) 191.
[24] T. Blasco, A. Corma, A. Martinez, P. Martinez-Escolano, J. Catal. 177 (1998) 306.
[25] I.V. Kozhevnikov, K.K. Kloetstra, A. Sinnema, H.W. Zhandbergen, H. van Bekkum, J. Mol. Catal. A: Chem. 114 (1996) 287.
[26] M. Kruk, M. Jaroniec, A. Sayari, Langmuir 13 (1997) 6267.
[27] E.P. Parry, J. Catal. 2 (1963) 371.
[28] M.L. Occelli, S. Biz, A. Auroux, G.J. Ray, Microporous Mesoporous Mater. 26 (1998) 193.
[29] C.A. Emeis, J. Catal. 141 (1993) 347.
[30] J.S. Beck, J.C. Vartuli, W.J. Roth, M.E. Leonowicz, C.T. Kiesge, K.D. Schmitt, C.T.-W. Chu, D.H. Olson, E.W. Sheppard, S.B. McCullen, J.B. Higgins, J.L. Schlenker, J. Am. Chem. Soc. 114 (1992) 10834.
[31] C.-Y. Chen, H.-X. Li, M.E. Davis, Microporous Mater. 2 (1993) 17.
[32] Y. Izumi, Memories of the School of Engineering Nagoya University, vol. 48, no. 2, 1996, pp. 194–234.
[33] Q.-Y. Liu, W.-L. Wu, J. Wang, X.-Q. Ren, Y.-R. Wang, Microporous Mesoporous Mater. 76 (2004) 51.
[34] A. Matsumoto, H. Chen, K. Tsutsumi, M. Grun, K. Unger, Microporous Mesoporous Mater. 32 (1999) 55.
[35] R. Mokaya, W. Jones, J. Catal. 172 (1997) 211.
[36] Z. Luan, C.-F. Cheng, H. He, J. Klinowski, J. Phys. Chem. 99 (1995) 10590.
[37] S. Hitz, R. Prins, J. Catal. 168 (1997) 194.
[38] V.M. Mastikhin, S.M. Kulikov, A.V. Nosov, I.V. Kozhevnikov, I.L. Mudrakovsky, M.N. Timofeeva, J. Mol. Catal. 60 (1990) 65.
[39] A. Corma, Chem. Rev. 95 (1995) 559.
[40] A. Sakthivel, S.K. Badamali, P. Selvam, Microporous Mesoporous Mater. 39 (2000) 457.

[41] K. Shanmugapriya, M. Palanichamy, B. Arabindoo, V. Murugesan, J. Catal. 224 (2004) 347.
[42] S.B. Pu, J.B. Kim, M. Seno, T. Inul, Microporous Mater. 10 (1997) 25.
[43] P.A. Jalil, N. Tabet, M. Faiz, N.M. Hamdan, Z. Hussain, Appl. Catal. A: Gen. 257 (2004) 1.
[44] M.T. Pope, Heteropoly and Isopoly Oxometalates, Springer, Berlin, 1983.
[45] I.V. Kozhevnikov, A. Sinnema, R.J.J. Jansen, K. Pamin, H. van Bekkum, Catal. Lett. 30 (1995) 241.
[46] A. Kukovecz, Z. Konya, I. Kirics, J. Mol. Struct. 563–564 (2001) 409.
[47] C. Rocchiccioli-Deltcheff, M. Fournier, R. Frank, R. Thouvenot, Inorg. Chem. 22 (1983) 207.
[48] J.A. Dias, E. Caliman, S.C.L. Dias, M. Paulo, A.T.C.P. de Souza, Catal. Today 85 (2003) 39.
[49] J.A. Dias, J.P. Osegovic, R.S. Drago, J. Catal. 183 (1999) 83.
[50] M. Karthik, A. Vinu, A.K. Tripathi, N.M. Gupta, M. Palanichamy, V. Murugesan, Microporous Mesoporous Mater. 70 (2004) 15.
[51] J.C. Vedrine, A. Auroux, P. Dejaifve, V. Ducarme, H. Hoser, S. Zhou, J. Catal. 173 (1982) 147.
[52] J.-S. Kim, J.-M. Kim, G. Seo, N.C. Park, H. Niiyama, Appl. Catal. 37 (1988) 45.
[53] B. Chakraborty, B. Viswanathan, Catal. Today 49 (1999) 253.
[54] M. Bhagiyalakshmi, K. Shanmugapriya, M. Palanichamy, B. Arabindoo, V. Murugesan, Appl. Catal. A: Gen. 267 (2004) 77.